On the estimate of earthquake magnitude at a local seismic network

Giuseppe Di Grazia [1], **Horst Langer** [1], **Andrea Ursino** [1], **Luciano Scarfì** [1] and **Stefano Gresta** [2]
[1] *Istituto Nazionale di Geofisica e Vulcanologia, Sezione di Catania, Priolo-Gargallo (SR), Italy*
[2] *Dipartimento di Scienze Geologiche, Università di Catania, Italy*

Abstract
We investigated possible uncertainties and biases of magnitude estimate arising from instrument characteristics, site conditions and routine data processing at a local seismic network running in Southeastern Sicily. Differences in instrument characteristics turned out to be of minor importance for small and moderate earthquakes. Magnitudes routinely calculated with the HYPOELLIPSE program are obtained from the peak ground velocities applying a correction for the dominant period. This procedure yields slightly lower values than the standard procedure, where magnitudes are estimated from peak ground displacement. In order to provide the operators in the data center with a tool for an immediate estimate of earthquake size from drum records we carried out a bivariate regression relating local magnitude (M_L) to the duration of the signal and the travel time difference of *P*- and *S*-waves.

Key words *Southeastern Sicily – digital seismic network – magnitude*

1. Introduction

In the context of seismic studies and surveillance, magnitude is the preferred measure for earthquake size, since it permits a straightforward comparison of events from different zones and depths. In response to practical needs, Richter (1935) proposed a magnitude scale based solely on amplitudes recorded on seismograms. Moving on from Wadati's (1931) analysis on the relation of peak amplitude of ground motion and earthquake distance, Richter took several bold steps to render the estimate of earthquake magnitude simple and easy to carry out. The Richter magnitude scale was originally developed with respect to local earthquakes in Southern California. Those events originated at depth not much different from 15 km so that effects due to the variations of focal depth could be widely neglected. Richter also skipped the tedious procedure of converting recorded seismograms into true ground motion. This because the Southern California Network was uniformly equipped with Wood-Anderson seismometers which have a uniform displacement amplification over a frequency range appropriate for most local earthquakes. The simplicity and robustness of Richter's local magnitude scale has made it the most commonly applied measure of earthquake energy in the framework of seismic surveillance with local networks. Typically, these networks are equipped with short period instruments with natural frequencies between 1 and 2 Hz and are devoted to the observation of small earthquakes at distances ranging from a few to no more than some hundreds of kilometers. The equipment of modern local seismic networks differs with some respect from the configuration used by Richter for the definition of the local magnitude (M_L). Seismometers may have a natural period and damping different from the

Mailing address: Dr. Stefano Gresta, Dipartimento di Scienze Geologiche, Università di Catania, Corso Italia 55, 95129 Catania, Italy; e-mail: gresta@mbox.unict.it

Wood-Anderson instrument, and their transfer function above the natural frequency is flat with respect to ground velocity rather than displacement. In such a way, the currently used procedures include deconvolution and convolution for the related instrumental curves (see, among others, the recent paper by Del Pezzo and Petrosino, 2001).

The aim of the present work is to investigate possible biases which may arise from the differences of local magnitude estimate under current conditions at the Southeastern Sicily seismic network with respect to the original situation at the time of Richter. In particular, we focus on the aspect of instrumental characteristics, and compare the standard magnitude estimates implemented in the HYPOELLIPSE code. Since the underground conditions vary from station to station we also investigate station dependent magnitude residuals.

The seismometer output in many networks (including the one considered in the present work) is proportional to ground velocity. Consequently, displacement amplitudes cannot be read directly from paper drum records. Furthermore, the paper recordings often concern the vertical component only, whereas the magnitude is estimated, by definition, from peak amplitudes on the horizontal components. For this reason, we carried out a bivariate regression for the estimate of local magnitude from signal duration and travel time differences of *P* and *S*-wave onsets as inferred from paper drum seismograms. This to provide a simple tool for an immediate magnitude estimate aimed at seismic surveillance.

2. Data analysis

The Southeastern Sicily Seismic Network (SESSN), currently run by the Istituto Nazionale di Geofisica e Vulcanologia (INGV), consists of 9 digital 3-component stations, each equipped with short period Mark L4-3D seismometers having a natural frequency of 2.0 Hz and a damping of *ca.* 65% of critical. Their calibration curves show a flat response in the frequency range between 2 and 160 Hz. The data are collected with a sampling frequency of 125 Hz; the corner frequency of the antialiasing filter is 51 Hz. The location of stations belonging to the network is shown in fig. 1.

2.1. *The role of instrument response*

The frequency content of the seismic signal crucially depends on spectral source parameters, in particular the corner frequency, which depends on the source size and stress drop. As the seismometer represents a high pass filter we expect that M_L-estimate is underestimated in particular for large earthquakes whose spectral content is dominated by low frequencies.

In order to discuss the role of instrumental response on magnitude estimate, we simulated a series of synthetic *SH*-seismograms for a half-space using Brune's (1970) source model. We varied the source radius r_0 from 100 m to 2000 m assuming a constant stress drop of 100 bars for all simulations and a source-receiver distance of 20 km. Besides geometrical spreading for body waves, we accounted for attenuation introducing band limiting effects by low-pass filtering the signal using a Butterworth filter with 2 filter sections and corner frequencies of 5 and 10 Hz, respectively. The physical origin of the high frequency band limitation is still unresolved (see, *e.g.*, Atkinson, 1996). Hanks (1982) claims that the frequently observed upper frequency limit – called f_{max} – in acceleration spectra or in displacement spectra of micro-earthquake recordings is an effect of wave propagation related to the competence of the near-surface material. On the other hand, if we interprete f_{max} in terms of a classical absorption law expressed by the term

$$e^{-\kappa\pi f}$$

where

$$\kappa = \int \frac{ds}{Q * C_s}$$

and C_s = shear wave velocity, Q = constant quality factor for *S*-waves, f = frequency (Hz), s = distance, then the limiting frequencies of 5 and 10 Hz correspond to $\kappa \approx 0.03$ and 0.015, respectively.

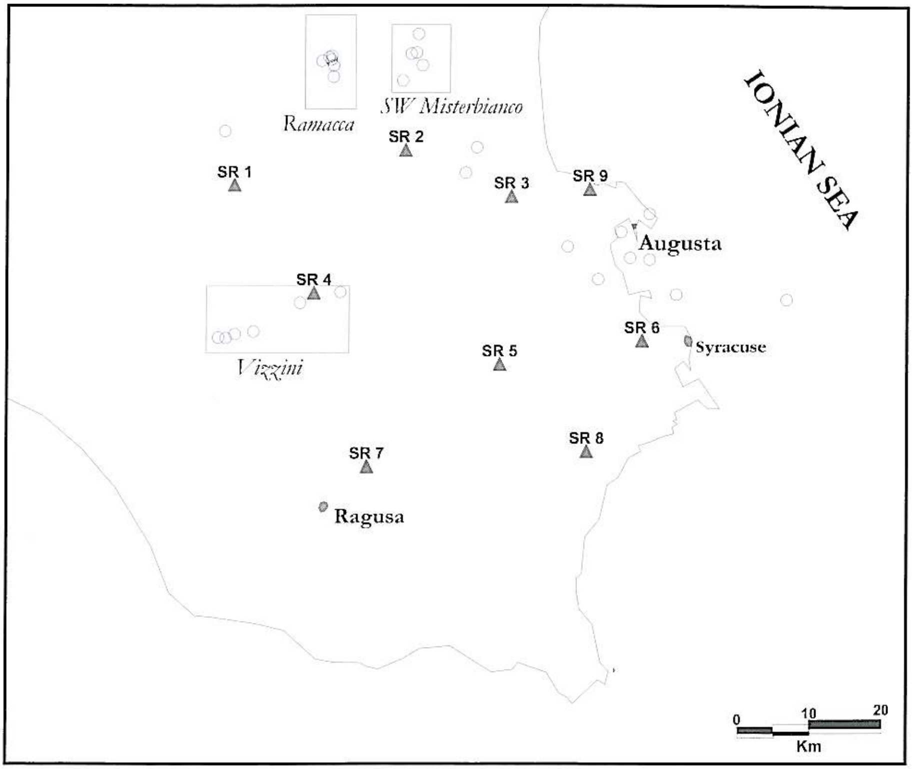

Fig. 1. Sketch map showing the seismic network and the epicentral distribution of the 29 local events composing the *dataset1* (see text for details).

All filtered traces were convoluted with the simulated instrument responses according to the characteristics of a Wood-Anderson instrument, a MarkL4-3D seismometer (the one currently used at all stations in Southeastern Sicily) and a hypothetical instrument with a natural frequency (f_s) of 0.7 Hz and a damping of 0.65 (see table I).

Table I. Parameters of the three discussed seismometers.

Instrument	f_s	Damping
Mark L4-3D	2.0	0.65
Wood-Anderson	1.25	0.8
Hypothetical	0.7	0.65

The resulting simulated local magnitudes shown in fig. 2 reproduce general trends which have been noted in observed data by various authors (*e.g.*, Hanks and Boore, 1984; Langer, 1990) and which can be described by the relation

$$M_L \propto r_0^n$$

where $r_0 = 1/f_0 = 0.372 * C_S * t_0$, t_0 = corner period shown in fig. 2 and C_S = shear wave velocity.

In the low-magnitude range we observe a rapid increase in magnitude according to a law with $n = 3$. Towards higher magnitudes, n decreases to a value of 2 in the range of moderate earthquakes and tends to zero for large earthquakes. The differences of M_L estimate between

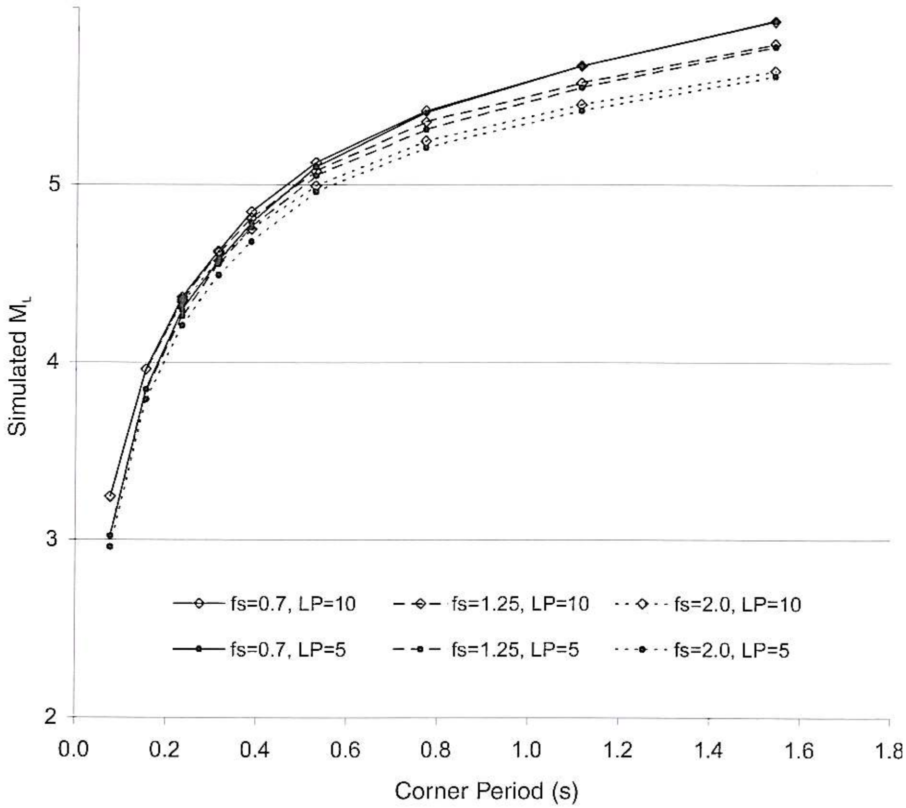

Fig. 2. Simulated magnitudes for various instrumental responses and high frequency cut-offs. Here *fs* is the natural frequency of the seismometer and *LP* is the corner frequency of the Butterworth low-pass filter.

the various instrument responses are more pronounced for larger magnitudes. As a general rule one observes that the estimated M_L is higher the lower the natural frequency of the seismometer. For instance, the difference between the Wood-Anderson seismometer and the MarkL4-3D one amounts to *ca.* 0.2 units for a corner period of the source of 1.8 s and reaches 0.35 when the Mark seismometer is compared to the hypothetical instrument with a natural frequency of 0.7 Hz.

The role of the instrument characteristics decreases with the corner period t_0 (see fig. 2). For magnitudes $M_L = 3$ or lower (which covers 99% of our data), the differences between the various instruments is at most 0.06 (in the case where $f_{max} = 5$ Hz). In our simulation $M_L = 3$ corresponds to a corner period of *ca.* 0.08 s. For this case, the differences introduced by the different low-pass effects, referring to the same instrument, range from 0.22 to 0.28, depending on the instrument characteristics. The curves obtained for the two values of f_{max} – keeping constant the instrumental characteristics – converge as corner periods and magnitudes increase. As mentioned earlier, these filters were introduced in order to emulate varying effects of wave propagation at the stations. However, no site dependent amplification factor has been accounted for, which could be represented roughly by a station correction constant in the magnitude estimate.

Table II. Magnitude residuals at various stations, average magnitudes (M_L) from peak displacement readings compared to average magnitudes (M_{LHE}) calculated by HYPOELLIPSE. The magnitude residuals at the single stations were calculated with respect to averages obtained from peak displacement amplitude readings. Data in italics refer to quarry blasts.

#	SR1	SR2	SR3	SR4	SR5	SR6	SR7	SR8	SR9	Eventcode	M_L	M_{LHE}
1	0.45	−0.35	0.05						−0.15	99110103	1.62	1.50
2	0.50	−0.45	0.20	−0.10	0.00				−0.15	99110105	2.60	2.20
3	0.45	−0.60	0.10						−0.05	99110106	1.70	1.00
4	0.70	−0.60	0.10	−0.10	−0.05				−0.05	99110107	2.85	2.20
5	0.80	−0.55	0.25		−0.10		−0.30		−0.10	99110109	2.10	1.60
6	0.70	−0.50	0.20	−0.15	−0.05		0.00		−0.10	99110110	2.50	1.90
7	*0.15*	*0.10*	*0.05*	*0.04*					*−0.34*	*99110121*	*1.63*	*1.30*
8		*0.07*	*0.09*		*0.04*			*0.07*	*−0.27*	*99110152*	*1.74*	*1.60*
9	0.30	0.00	0.00				−0.20		−0.10	99070008	2.10	1.60
10	0.05	0.10	0.35		−0.10	−0.45	0.05			99070017	1.65	0.90
11	−0.07	0.02	0.19		0.06	−0.05	−0.12		−0.03	99080021	1.39	1.10
12	0.17	0.09	−0.27		0.01					99110080	1.14	1.00
13	0.41	0.23	−0.27	−0.57					0.10	99110083	1.19	1.30
14	0.38	−0.08	−0.57		0.02		0.18		0.07	99110085	1.22	1.50
15	0.39	0.15	−0.26		−0.20				−0.08	99110094	1.68	1.30
16		0.11	0.16		0.15	−0.44	0.41		−0.39	99090144	1.16	1.10
17	0.51	−0.21	−0.18	−0.03	0.16	−0.10			−0.15	99100103	3.32	3.10
18		−0.29	0.20		0.18	−0.03			−0.06	99100006	0.93	0.70
19	0.40	−0.07				0.15			−0.48	99110018	1.71	1.40
20			0.03			−0.03				99110026	1.39	1.50
21	*0.48*	*−0.45*	*−0.12*		*0.23*	*0.04*	*−0.18*			*99100033*	*1.32*	*1.30*
22		*0.00*	*0.10*			*−0.10*				*99100036*	*1.01*	*0.90*
23			*−0.21*		*0.27*	*−0.06*				*99100039*	*1.24*	*0.90*
24		*−0.23*	*−0.02*		*0.29*	*0.19*	*−0.23*			*99100035*	*1.64*	*1.80*
25	0.33	−0.28	−0.13		0.32	−0.25			0.01	99090285	1.83	1.60
26	0.38	0.10	−0.45		0.03		0.14		−0.20	99070007	1.45	1.30
27	0.15	−0.09	−0.26	0.10	0.14	−0.21	0.28		−0.11	99070011	1.55	1.20
28	0.31	−0.05	−0.19				0.20		−0.27	99070012	1.16	0.90
29	0.30	−0.15	−0.12		0.16	−0.23			0.04	99100102	1.72	1.40
	0.37	−0.15	−0.03	−0.12	0.12	−0.11	−0.00	0.07	−0.11	Average residuals over all events		
	0.20	0.25	0.22	0.20	0.16	0.18	0.24		0.15	Standard deviation of residuals		
					Average residuals							
	0.60	−0.51	0.15	−0.12	−0.05		−0.15		−0.08	Ramacca zone (#1-#6)		
	0.23	0.07	−0.10	−0.57	0.14	−0.25	−0.02		−0.02	Vizzini zone (#9-#15)		
	0.43	−0.22	−0.04	−0.03	0.24	−0.02	−0.33		−0.15	Augusta-Syracuse zone(#17-#25)		
	0.29	−0.05	−0.26	0.10	0.11	−0.22	0.21		−0.09	SW Misterbianco zone (#26-#29)		

The general trends of magnitude and geometrical source parameters can be understood in a straightforward way (see Hanks and Boore, 1984). For higher magnitudes, one expects source spectra to be rich in low frequencies. Consequently the changes these signals undergo are more severe as the natural frequency of the seismometer increases. On the other hand, the existence of a high frequency limit f_{max} has a significant influence on the signals of small earthquakes. In fact, the lower f_{max}, the lower the estimated magnitude, particularly of small earthquakes.

2.2. *Magnitude estimate and residuals*

As a first step, we selected 29 local events (reported in table II and fig. 1, hereafter quoted as *dataset1*). Magnitudes were estimated following the standard procedure as proposed by Lee and Stewart (1981). This consists in: i) converting the velocity seismograms in ground displacement after carrying out a base-line correction in order to remove low-frequency noise; ii) picking maximum trace amplitudes on both horizontal components and averaging the two values; iii) applying the correction values for source-receiver distance from Richter's (1958) table. As the epicenters of the considered events are commonly close to the seismic stations (typically between 20 and 60 km), we used hypocentral distances rather than the epicentral ones to avoid a severe underestimation of the wavepath length.

Alternatively to the use of Richter's table, one can roughly estimate the correction values for distance using a formula like

$$M_L = \log(2800 \cdot U_{max}[\text{mm}]) - a + b \cdot \log(s[\text{km}])$$

replacing Richter's distance correction by the relation

$$-a + b \cdot \log(s[\text{km}])$$

where: $a = 0.15$ for $s < 200$ km and $a = 3.38$ for $s \geq 200$ km; $b = 1.6$ for $s < 200$ km and $b = 3.0$ for $s \geq 200$ km; s being the hypocentral distance. This is the routine implemented in the HYPOELLIPSE program (Lahr, 1989). Discrepancies with respect to the original form by Richter are indeed less than 0.2 in the whole distance range (see fig. 3).

The comparison of estimated magnitudes at the 9 stations of the SESSN reveals significant biases at certain sites, in particular at SR1 station. Over the whole *dataset1* magnitudes at SR1 station tend to be overestimated by 0.37 units (see table II). On the other hand, the magnitudes estimated at SR2 have been, on average, underestimated by 0.15 units. These biases may be attributed either to station site conditions or to the geometrical source-receiver configuration.

For instance, the residuals at SR1 obtained for the Ramacca sequence (events # 1-6 in table II) are particularly high, whereas we note very low amplitudes at SR2. These events, however, are clustered closely together, and they follow the same focal mechanism (Scarfì *et al.*, 2001). Indeed, the residuals at SR1 are minor for the events from other azimuths, and become practically insignificant at SR2.

In the HYPOELLIPSE program, magnitudes are estimated from ground velocity seismograms. Peak ground displacements are estimated by applying a correction according to the dominating frequency during a selected part of the signal (for details see Lahr, 1989) instead of carrying out a formal integration of the seismogram, which would require some additional preprocessing steps in order to eliminate long period noise.

Compared to the standard procedure, however, magnitudes obtained from the output of HYPOELLIPSE seem to be underestimated. This trend is clearer if we consider three key stations (*i.e.*, SR2, SR3 and SR9) which show minor residuals and where more data are available. In fig. 4 we compare magnitude estimates using the two methods for a second data set of 37 events (hereafter *dataset2*) with epicentral distances ranging from *ca.* 20 to 120 km (fig. 5). A rough correction is obtained from the averages of the three key stations as

$$M_{LHE} = 1.04 \cdot M_L - 0.25$$

where M_{LHE} is the magnitude calculated with

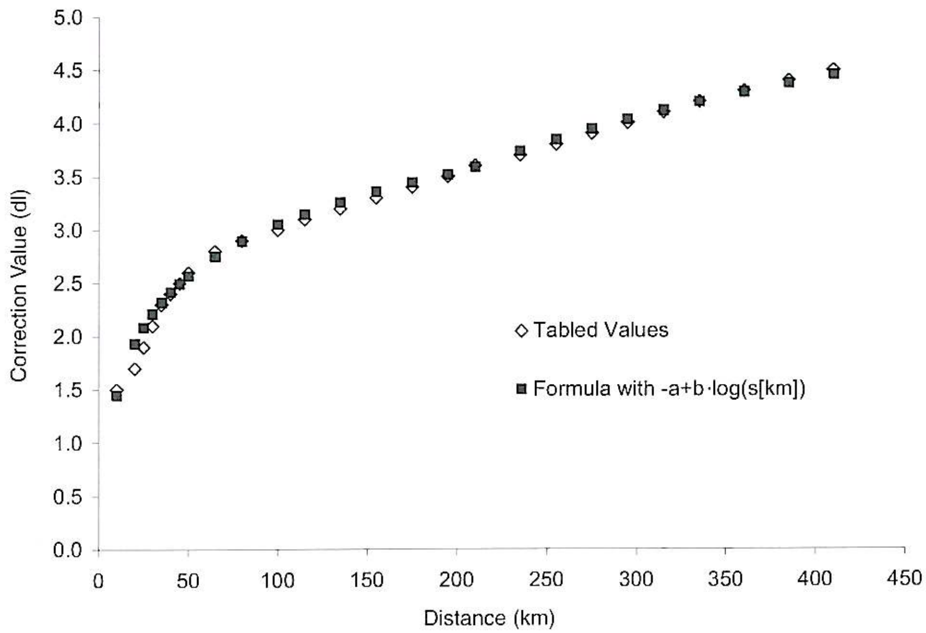

Fig. 3. Distance correction used for the estimation of M_L (see text for details).

HYPOELLIPSE and M_L is the one obtained following the standard procedure.

Jennings and Kanamori (1983) recommend some caution when local magnitudes are determined at small epicentral distances. Indeed, the original curve by Richter (1935) was established for distances larger than 25 km, and the extension by Gutenberg and Richter (1942) to distances between 0 and 30 km is based on an instrument whose characteristics differ significantly from the standard Wood-Anderson seismograph. A further problem tackled by Jennings and Kanamori (1983), *i.e.* the geometrical extension of the seismic source and the definition of a suitable source-receiver distance, is of little importance in our context as the expected source dimensions of earthquakes discussed here are small compared to the hypocentral distances.

The effect of using the distance correction proposed by the above mentioned authors (see fig. 6) is minor in *dataset2*. One reason relies on the fact that we use distances defined relative to the hypocenters instead of the epicenters. Since our events have focal depth typically around 15 to 20 km (fig. 7), most of the distances fall in ranges where the deviations with respect to Richter's distance correction are limited. In fact, comparing magnitude estimates using Richter's original values and those obtained by applying the modifications proposed by Jennings and Kanamori (1983), we find (see fig. 8) rather small deviations in the order of *ca.* 0.05 units. Also in *dataset1*, which represents local events recorded at smaller distances, the differences between Richter's original values and those given by Jennings and Kanamori are essentially below 0.05 for tectonic earthquakes. Differences up to 0.2 units are observed for the quarry blasts. Besides the limited differences, the application of these modifications to our data is questionable since the foci of the earthquakes considered here are deeper than in the data set used by Jennings and Kanamori (1983), and – as these authors point out – the deviations of magnitude estimates are expected to decrease with increasing focal depth.

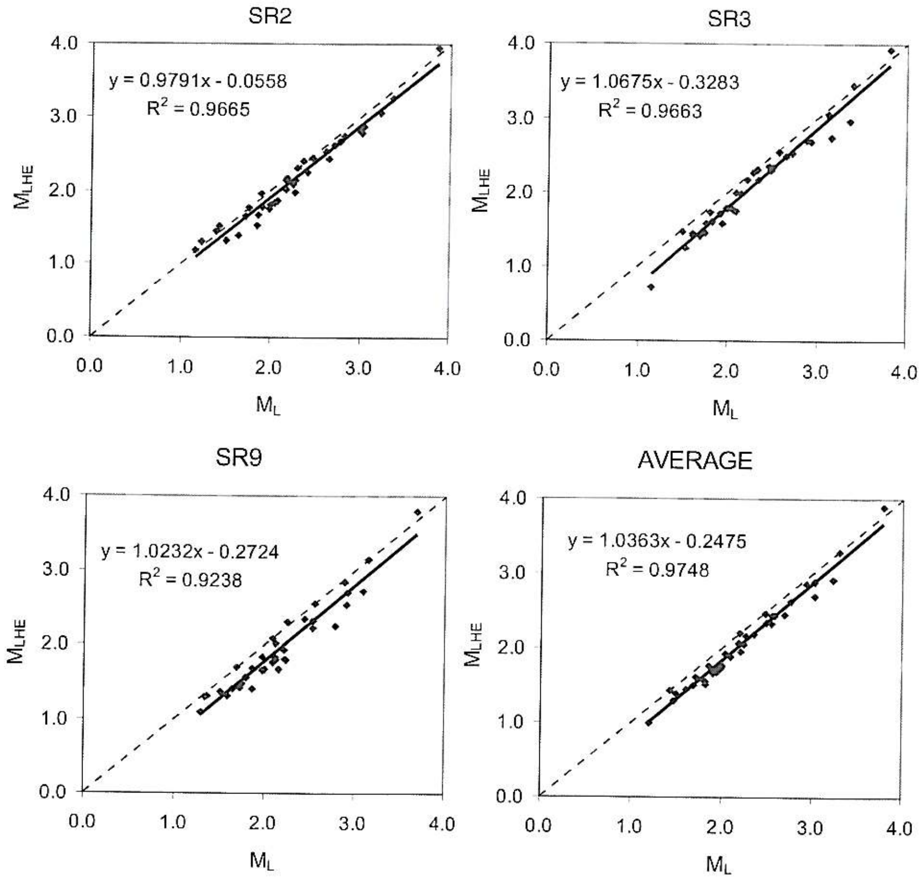

Fig. 4. Comparison of the local magnitude calculated by HYPOELLIPSE (M_{LHE}) with respect to the one obtained with the standard procedure (M_L), for the 37 events of *dataset2*. Results are shown for each of the three key stations and for their average values.

The distance correction of local magnitude estimates depends on the individual attenuation laws of an earthquake zone. We simulated synthetic wave packages following a stochastic approach recently presented by Del Pezzo and Petrosino (2001), assuming a constant Q of 300 together with a shear wave velocity of 3.5 km/s. For the sake of simplicity, we supposed that the crustal model corresponds to a semi-infinite half-space. The spectral characteristics for the seismic source were accounted for by applying a shaping filter to the random sequence according to an ω^2-model with a corner frequency of 5 Hz.

From the synthetic data we obtained a relation according to

$$M_L =$$

$$= \log(2800 \cdot U_{max}[\mathrm{mm}]) + 1.27 \cdot \log(s[\mathrm{km}]) + a$$

being valid for distances < 100. The constant a is obtained by choosing a reference distance and equating with Lahr's (1989) formula (distances < 200 km)

$$M_L = \log(2800 \cdot U_{max}[\mathrm{mm}] + 1.6 \cdot \log(\mathrm{s}[\mathrm{km}]) - 0.15.$$

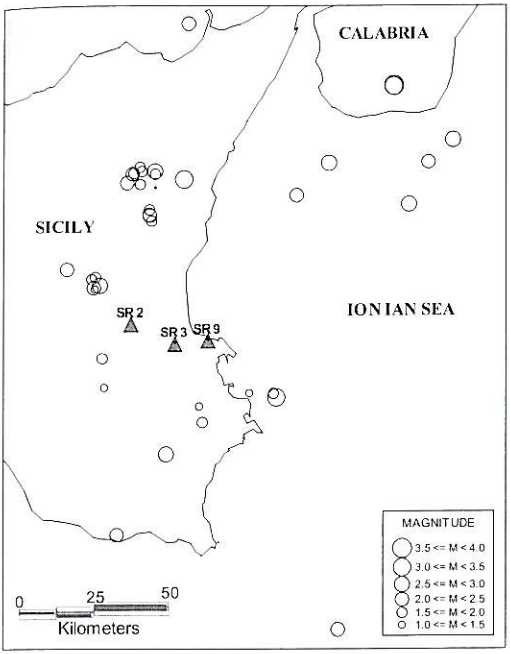

Fig. 5. Location of the three key stations (see text for details) and epicentral distribution of the events of *dataset2*.

With a reference distance of 40 km (the most frequent distance in our two data sets) we obtain $a = 0.377$. Thus the difference between the magnitudes calculated with the relation from synthetic data and those obtained with Lahr's formula is about 0.1 units at a distance of 20 km whereas the two formulae differ by -0.15 units for a distance of 120 km. On the whole, however, as magnitudes are calculated from the average of stations at various distances, the differences between the two formulae turns out to be smaller, *i.e.* -0.04 ± 0.06 units in *dataset2* and 0.04 ± 0.06 in *dataset1*.

2.3. *Duration magnitude*

Drum records on paper are still a widely used tool for seismic monitoring purposes. This happens at our operative center, too. However, seismograms on paper are proportional to the ground velocity rather than to the displacement. On the paper recordings with a speed of 60 mm/s the time resolution is not sufficiently high to estimate dominating frequencies which could be used, similarly to the technique used in HYPOELLIPSE, for a conversion of peak ground velocity amplitudes to those in terms of ground displacement. Moreover, in our specific case, paper recordings are available only for the vertical component, whereas local magnitudes are estimated from the horizontal component seismograms. Nonetheless, it is desirable to provide the operators of the operative center with a tool for an immediate estimate of earthquake size. We therefore carried out a bivariate regression relating local magnitude to the duration of the signal τ and the travel time difference $(t_s - t_p)$ between *P*- and *S*-waves. When reading the relevant parameters $(t_s - t_p)$ and τ we tried to emu-

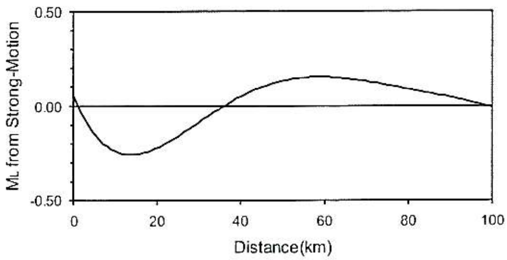

Fig. 6. Interpolated curve of differences between magnitude estimation with revised attenuation curve (Jennings and Kanamori, 1983) and standard attenuation curve (Richter, 1935, 1958).

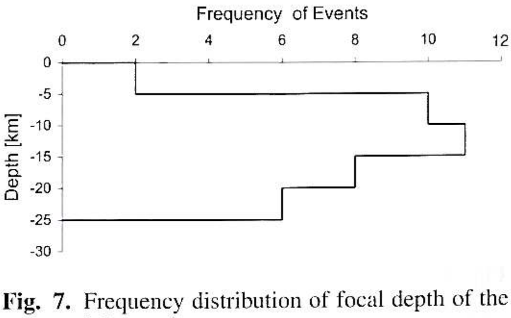

Fig. 7. Frequency distribution of focal depth of the events of *dataset2*.

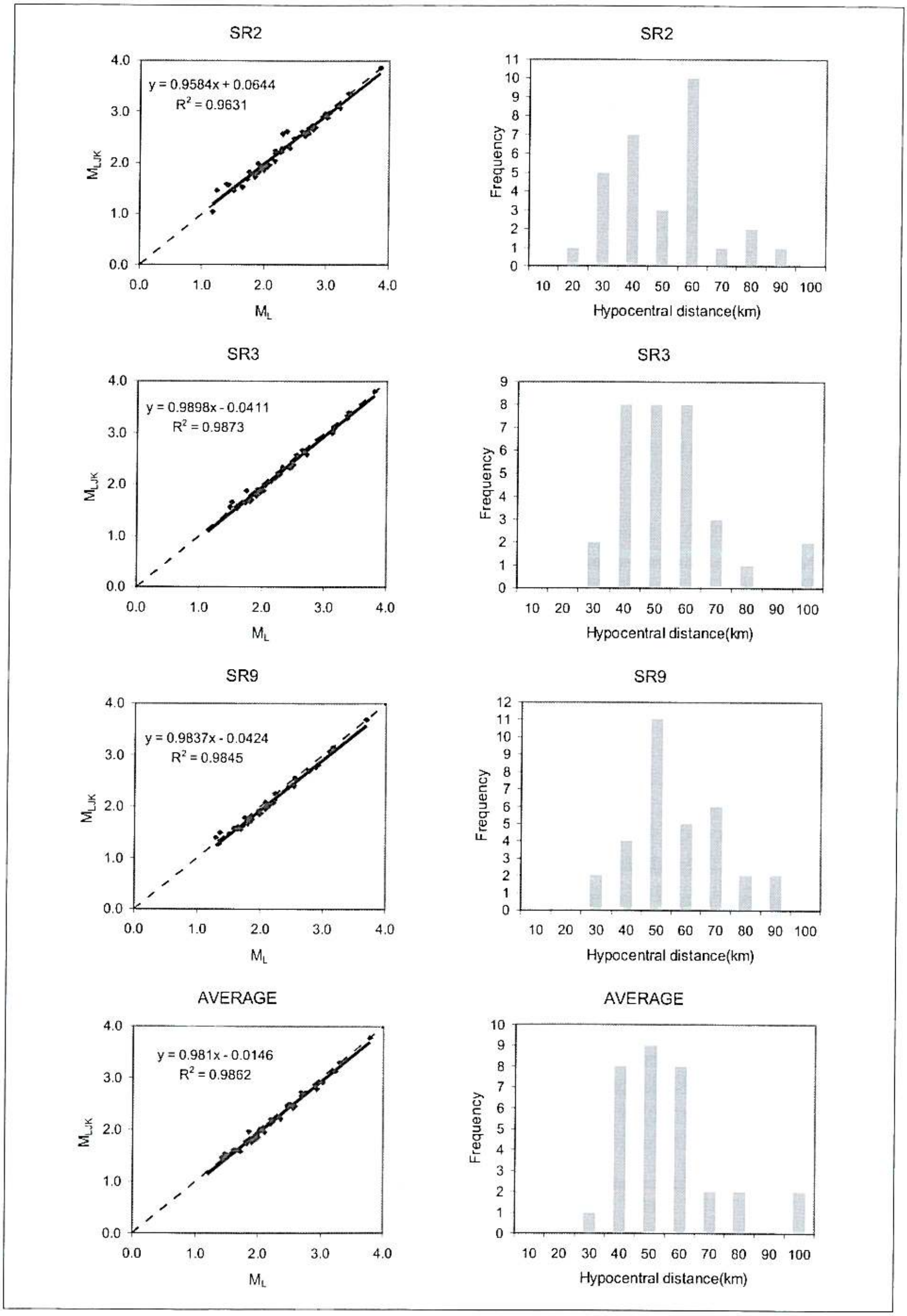

Fig. 8. *Left*: comparison of the local magnitude (M_{LJK}) obtained with revised attenuation curve by Jennings and Kanamori (1983) with respect to the one obtained with the standard procedure (M_L). *Right*: frequency distribution of the hypocentral distance.

Table III. Coefficients for the estimation of magnitude from signal duration and travel time difference of *P*- and *S*-waves.

Station	a	b	c	Standard dev. (M)	Goodness of fit R^2
SR2	– 1.26 ± 0.33	1.98 ± 0.23	0.03 ± 0.01	± 0.29	0.79
SR3	– 1.77 ± 0.30	2.25 ± 0.22	0.03 ± 0.02	± 0.27	0.85
SR9	– 1.26 ± 0.23	1.86 ± 0.17	0.04 ± 0.01	± 0.22	0.86

Table IV. Estimation of magnitudes from signal duration and travel time difference of *P*- and *S*-waves.

	↓Duration (s) / t_s-t_p (s)→	2	3	4	5	7	10	15	20
SR2	10	0.8	0.8	0.8	0.9	0.9			
	15	1.1	1.2	1.2	1.2	1.3	1.4		
	20	1.4	1.4	1.4	1.5	1.5	1.6	1.8	
	25	1.6	1.6	1.6	1.7	1.7	1.8	2.0	2.1
	30	1.7	1.8	1.8	1.8	1.9	2.0	2.1	2.3
	40	2.0	2.0	2.0	2.1	2.1	2.2	2.4	2.5
	50	2.2	2.2	2.2	2.3	2.3	2.4	2.5	2.7
	70	2.5	2.5	2.5	2.5	2.6	2.7	2.8	3.0
	100	2.8	2.8	2.8	2.8	2.9	3.0	3.1	3.3
	150	3.1	3.1	3.2	3.2	3.3	3.3	3.5	3.6
	200	3.4	3.4	3.4	3.4	3.5	3.6	3.7	3.9
SR3	10	0.5	0.6	0.6	0.6	0.7			
	15	0.9	1.0	1.0	1.0	1.1	1.2		
	20	1.2	1.3	1.3	1.3	1.4	1.5	1.7	
	25	1.4	1.5	1.5	1.5	1.6	1.7	1.9	2.0
	30	1.6	1.7	1.7	1.7	1.8	1.9	2.0	2.2
	40	1.9	1.9	2.0	2.0	2.1	2.2	2.3	2.5
	50	2.1	2.2	2.2	2.2	2.3	2.4	2.5	2.7
	70	2.4	2.5	2.5	2.5	2.6	2.7	2.9	3.0
	100	2.8	2.8	2.9	2.9	3.0	3.1	3.2	3.4
	150	3.2	3.2	3.3	3.3	3.4	3.5	3.6	3.8
	200	3.5	3.5	3.5	3.6	3.6	3.7	3.9	4.1
SR9	10	0.7	0.7	0.8	0.8	0.9			
	15	1.0	1.1	1.1	1.1	1.2	1.3		
	20	1.2	1.3	1.3	1.4	1.4	1.6	1.8	
	25	1.4	1.5	1.5	1.5	1.6	1.7	1.9	2.1
	30	1.6	1.6	1.7	1.7	1.8	1.9	2.1	2.3
	40	1.8	1.8	1.9	1.9	2.0	2.1	2.3	2.5
	50	2.0	2.0	2.1	2.1	2.2	2.3	2.5	2.7
	70	2.3	2.3	2.3	2.4	2.5	2.6	2.8	3.0
	100	2.5	2.6	2.6	2.7	2.7	2.9	3.1	3.3
	150	2.9	2.9	3.0	3.0	3.1	3.2	3.4	3.6
	200	3.1	3.1	3.2	3.2	3.3	3.4	3.6	3.8

late the conditions under which some operators would proceed. First, we defined the noise level from the trace amplitude prior to the event. We then measured the duration as the interval from the first onset to the time where the signal visually fell below the noise level.

Among the 9 stations of the SESSN, we again chose SR2, SR3 and SR9 as key stations and carried out the regression using the *dataset2*. The magnitudes we have been using are the ones obtained by the procedure of HYPOELLIPSE for the single station, since these are the ones usually reported in our seismic bulletin. The coefficients of the regression

$$y = a + bx_1 + cx_2$$

where y is M_{LHE} obtained for the considered station, x_1 corresponds to $\log_{10}(\tau[s])$ and x_2 to $(t_s - t_p)$ $[s]$ and the coefficients a, b, c, are given in table III.

The travel time difference $(t_s - t_p)$ is a measure for the source distance s. Assuming a P-wave velocity of 6 km/s and a relation of P- and S-wave velocities of 1.8 (Amato *et al.*, 1995), we obtain s [km] $= 7.5 \cdot (t_s - t_p)$. For an immediate assessment of earthquake magnitude from drum recordings at our operative center, we propose the values given in table IV valid for the three key stations.

3. Conclusions

We have analyzed the accuracy of magnitude estimates at the Southeastern Sicily seismic network both from the view point of instrumental response and technical aspects. For small and medium earthquakes using MarkL4-3D seismometers, whose characteristics deviate from the Wood-Anderson instrument, the errors should be less than 0.1 units for magnitude 3 or smaller earthquakes, which represent 99% of our data. Magnitude estimates may be influenced by site effects, which may significantly limit the bandwidth of microearthquakes and introduce biases, for example, by soil amplification. We have evidenced those biases in particular at station SR1, where we obtained a systematic overestimation of magnitudes of on average 0.3 units.

For the sake of simplicity, the routine procedure of magnitude determination implemented on HYPOELLIPSE uses a rough approximation for converting peak ground velocity amplitudes to peak amplitudes of displacement. We compared the magnitude estimates of 37 events, for three key stations, obtained with HYPOELLIPSE and those following the standard procedure. The HYPOELLIPSE procedure gives slightly lower values than the standard technique (fig. 4). A rough correction was made using a simple relation. The problems reported by Jennings and Kanamori (1983) with the use of Richter's distance correction at local scale were found to be of minor importance as we use distances measured with respect to hypocenters instead of epicenters, and in our case, distances fall typically in ranges where the modifications are limited. Furthermore, as the focal depth of the events here considered are larger than those discussed by Jennings and Kanamori (1983), the possible biases encountered with Richter's distance correction can be neglected. The distance correction obtained from a synthetic simulation using an attenuation law of $Q = 300$ differs to some degree from the one used by Lahr (1989). Nonetheless, average magnitude estimates seem to be little affected by these differences.

For the practical purpose of an immediate assessment of earthquake size we established relations for the estimation of magnitudes from signal duration and the travel time differences of P- and S-waves. Slight differences were observed among three chosen key stations.

Acknowledgements

We are grateful to Edoardo Del Pezzo and Paolo Gasperini for their constructive criticism that strongly improved the early version of this paper.

REFERENCES

AMATO, A., R. AZZARA, A. BASILI, C. CHIARABBA, M. COCCO, M. DI BONA and G. SELVAGGI (1995): Main shock and aftershocks of the December 13, 1990, Eastern Sicily earthquake, *Ann. Geofis.*, **38** (2), 255-266.

ATKINSON, G.M. (1996): The high-frequency shape of the source spectrum for earthquakes in Eastern and Western Canada, *Bull. Seismol. Soc. Am.*, **86/1A**, 106-112.

BRUNE, J. (1970): Tectonic stress and the spectra of seismic shear waves from earthquakes, *J. Geophys. Res.*, **75**, 4997-5009.

DEL PEZZO, E. and S. PETROSINO (2001): A local magnitude scale for Mt. Vesuvius from synthetic Wood-Anderson seismograms, *J. Seismol.*, **5**, 207-215.

GUTENBERG, B. and C.F. RICHTER (1942): Earthquake magnitude, intensity, energy, and acceleration, *Bull. Seismol. Soc. Am.*, **32**, 163-191.

HANKS, T. (1982): f_{max}, *Bull. Seismol. Soc. Am.*, **72**, 1867-1879.

HANKS, T. and D. BOORE (1984): Moment-magnitude relations in theory and practice, *J. Geophys. Res.*, **89**, 6229-6235.

JENNINGS, P.C. and H. KANAMORI (1983): Effects of distance on local magnitudes found from strong-motion records, *Bull. Seismol. Soc. Am.*, **73**, 265-280.

LAHR, J.C. (1989): HYPOELLIPSE/version 2.0: a computer program for determining local earthquake hypocentral parameters, magnitude, and first motion pattern, *U.S. Geol. Surv., Open File Rep.*, 89/116, pp. 81.

LANGER, H. (1990): Input parameters for estimating seismic loading, *Nat. Hazards*, **3**, 125-139.

LEE, W. and S. STEWART (1981): Principles and applications of microearthquake networks, in *Advances in Geophysics* (Academic Press), Suppl. 2, pp. 293.

RICHTER, C. (1935): An instrumental earthquake magnitude scale, *Bull. Seismol. Soc. Am.*, **25**, 1-32.

RICHTER, C. (1958): *Elementary Seismology* (Freeman and Company, San Francisco), pp. 768.

SCARFÌ, L., H. LANGER, G. DI GRAZIA, A. URSINO and S. GRESTA (2001): Analysis of two swarms of microearthquakes in Southeastern Sicily: evidence for active faults?, *Ann. Geofis.* (in print).

WADATI, K. (1931): Shallow and deep earthquakes, *Geophys. Mag*, **4**, 231-283.

(received January 10, 2001;
accepted June 12, 2001)